

# Focused ion beam milling of optical films with complex surfaces at the subnanometer scale

K.-T. Liao <sup>a, b</sup>, J. Schumacher <sup>a</sup>, H. J. Lezec <sup>a</sup>, S. M. Stavis <sup>a, c</sup>

<sup>a</sup> *Center for Nanoscale Science and Technology, National Institute of Standards and Technology, Gaithersburg, MD 20899, USA.*

<sup>b</sup> *Maryland Nanocenter, University of Maryland, College Park, MD 20742, USA.*

<sup>c</sup> *samuel.stavis@nist.gov*

Structure–property relationships are fundamental to functional nanostructures of all dimensionalities, including surfaces, films, and slits with nanoscale vertical dimensions and microscale lateral dimensions. At EIPBN 2014, we introduced the focused ion beam (FIB) milling of complex surfaces in silicon (Si) with one nanometer vertical resolution.<sup>1</sup> At EIPBN 2015, we reported the FIB milling of Si and replica molding of polydimethylsiloxane (PDMS) with subnanometer vertical resolution.<sup>2</sup> Here, we demonstrate the FIB milling of complex surfaces in submicrometer films of silicon dioxide (SiO<sub>2</sub>) and silicon nitride (Si<sub>3</sub>N<sub>4</sub>) with subnanometer vertical resolution. These dielectric films have unique milling responses and show structural colors as an optical property. Our new patterning capability enables the rapid prototyping of complex films in dielectric materials with novel structure–property relationships for optical applications.

Submicrometer films of SiO<sub>2</sub> and Si<sub>3</sub>N<sub>4</sub> respond differently to a focused beam of gallium ions (Ga<sup>+</sup>) than bulk Si, resulting in some advantages for structural control at the subnanometer scale. At low doses, SiO<sub>2</sub> does not swell (Fig. 1a inset), unlike Si,<sup>2</sup> facilitating the FIB milling of subnanometer structures. In contrast, Si<sub>3</sub>N<sub>4</sub> swells more than Si (Fig. 1e inset) and also shows an inverted response to modulation of low dose by pass number and dwell time,<sup>2</sup> requiring additional calibration and FIB milling to return to the zero plane. As dose increases, both SiO<sub>2</sub> and Si<sub>3</sub>N<sub>4</sub> show a more complex milling response than Si,<sup>2</sup> which is approximately linear. SiO<sub>2</sub> and Si<sub>3</sub>N<sub>4</sub> show an approximately piecewise linear response, which still allows for facile calibration in discrete ranges of depth approximately from 0.1 nm to 10 nm and from 10 nm to 100 nm (Figs. 1a, 1e). The surface roughness of both materials remains approximately constant in a range from 0.3 nm to 0.6 nm for all milled depths (Figs. 1b, 1f), unlike the non-monotonic response of Si.<sup>2</sup> This response allows for consistent structural control across the nanoscale. Test patterns of SiO<sub>2</sub> and Si<sub>3</sub>N<sub>4</sub> show structural colors under illumination with white light (Figs. 1c–1h). This optical property is useful for interferometry of film thickness with high throughput in nanomanufacturing. Many other applications would also benefit from subnanometer control over the thickness of dielectric films, such as guiding light over surfaces, enhancing optoelectronic output, and tuning cathodoluminescent response.

---

<sup>1</sup> Total Nanofluidic Confinement Devices Nanofabricated by Focused Ion Beam Milling, K.-T. Liao, J. Schumacher, S. M. Stavis, EIPBN 2014

<sup>2</sup> FIB Milling and Replica Molding of Complex Surfaces with Atomic-Scale Precision, K.-T. Liao, J. Schumacher, H. J. Lezec, S. M. Stavis, EIPBN 2015

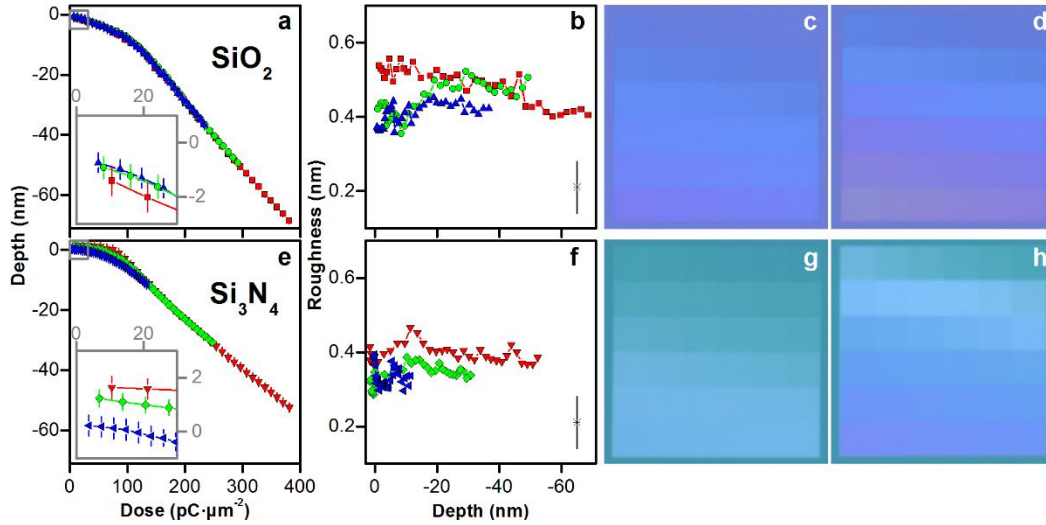


**Fig. 1.** Focused ion beam milling of optical films with complex surfaces at the subnanometer scale. **(a)** Atomic force microscopy (AFM) results showing the response of an  $\text{SiO}_2$  film with an initial thickness of  $\approx 500$  nm, thermally oxidized into a silicon (Si) substrate, to a variable dose of  $\text{Ga}^+$  from a FIB with an energy of 30 keV. At low doses, amorphous  $\text{SiO}_2$  does not swell, unlike crystalline  $\text{Si}$ ,<sup>2</sup> facilitating structural control. As dose increases, the response of  $\text{SiO}_2$  becomes approximately piecewise linear. **(b)** AFM results showing that the root-mean-square (RMS) surface roughness of  $\text{SiO}_2$  stays approximately constant at  $\approx 0.5$  nm, unlike  $\text{Si}$ ,<sup>2</sup> allowing consistent structural control across the nanoscale. The lone data marker in the lower right corner shows a representative value of uncertainty. All values of uncertainty are confidence intervals of 95 %. A future report will describe the details of uncertainty evaluation. **(c)** Brightfield optical micrograph (BOM) showing the test pattern corresponding to the blue data in (a, b). **(d)** BOM showing the test pattern corresponding to the red data in (a, b) Test patterns show structural colors under illumination with white light, which will be useful for optical analysis of film thickness with high throughput in a nanomanufacturing process. **(e)** AFM results showing the response of a film of stoichiometric silicon nitride ( $\text{Si}_3\text{N}_4$ ) with an initial thickness of  $\approx 400$  nm, deposited by low pressure chemical vapor deposition onto a Si substrate, to a variable dose of  $\text{Ga}^+$ . At low doses,  $\text{Si}_3\text{N}_4$  swells significantly. Further, in comparison to both Si and  $\text{SiO}_2$ ,  $\text{Si}_3\text{N}_4$  shows an inverted initial response to modulating the dose by increasing the dwell time and number of passes of the FIB.<sup>2</sup> A future report will elucidate these effects, which require additional calibration and milling to return to the zero plane. As dose increases, the response of  $\text{Si}_3\text{N}_4$  becomes approximately piecewise linear. **(f)** AFM results showing that the RMS surface roughness of  $\text{Si}_3\text{N}_4$  stays approximately constant at  $\approx 0.4$  nm across the nanoscale, unlike  $\text{Si}$ ,<sup>2</sup> allowing consistent structural control across the nanoscale. Tensile stress in  $\text{Si}_3\text{N}_4$  may result in the smoothest milled surface. **(g)** BOM showing the test pattern corresponding to the blue data in (e, f). **(h)** BOM showing the test pattern corresponding to the red data in (e, f). Test patterns show structural colors under illumination with white light.